Cell

Astrocytes Are Endogenous Regulators of Basal Transmission at Central Synapses

Aude Panatier,[1,2,4] Joanne Vallée,[1,2] Michael Haber,[3] Keith K. Murai,[3] Jean-Claude Lacaille,[1,2,*] and Richard Robitaille[1,2,*]
[1]Département de physiologie
[2]Groupe de Recherche sur le Système Nerveux Central
Université de Montréal, PO Box 6128, Station Centre-Ville, Montreal, QC H3C 3J7, Canada
[3]Centre for Research in Neuroscience, Department of Neurology and Neurosurgery, The Research Institute of the McGill University Health Centre, Montreal General Hospital, Montreal, QC H3G 1A4, Canada
[4]Present address: Neurocentre Magendie and Interdisciplinary Institute for Neuroscience, 146 Rue Léo Saignat, 33077 Bordeaux Cedex, France
*Correspondence: jean-claude.lacaille@umontreal.ca (J.-C.L.), richard.robitaille@umontreal.ca (R.R.)
DOI 10.1016/j.cell.2011.07.022

SUMMARY

Basal synaptic transmission involves the release of neurotransmitters at individual synapses in response to a single action potential. Recent discoveries show that astrocytes modulate the activity of neuronal networks upon sustained and intense synaptic activity. However, their ability to regulate basal synaptic transmission remains ill defined and controversial. Here, we show that astrocytes in the hippocampal CA1 region detect synaptic activity induced by single-synaptic stimulation. Astrocyte activation occurs at functional compartments found along astrocytic processes and involves metabotropic glutamate subtype 5 receptors. In response, astrocytes increase basal synaptic transmission, as revealed by the blockade of their activity with a Ca^{2+} chelator. Astrocytic modulation of basal synaptic transmission is mediated by the release of purines and the activation of presynaptic A_{2A} receptors by adenosine. Our work uncovers an essential role for astrocytes in the regulation of elementary synaptic communication and provides insight into fundamental aspects of brain function.

INTRODUCTION

Information is transmitted at synapses between neurons in the nervous system. Beyond the importance of neurons, evidence indicates that astrocytes, a type of glial cell, also contribute to information processing in the brain. Indeed, astrocytes detect neurotransmitters released during intense and sustained neuronal network activity (Fellin et al., 2004; Latour et al., 2001; Pasti et al., 1997) and, in turn, modulate synaptic transmission (Fellin et al., 2004; Henneberger et al., 2010; Panatier et al., 2006; Pascual et al., 2005; Pasti et al., 1997; Perea and Araque, 2005; Serrano et al., 2006) by releasing neuroactive substances termed gliotransmitters (e.g., purines, D-serine, and glutamate) (Halassa and Haydon, 2010; Volterra and Meldolesi, 2005). The regulation of synapses by astrocytes is largely based on intracellular Ca^{2+}-dependent processes and results from receptor activation, in particular, group I metabotropic glutamatergic receptors (mGluR) (Cai et al., 2000; D'Ascenzo et al., 2007; Fellin et al., 2004; Honsek et al., 2010; Porter and McCarthy, 1996). From this emerged the concept of the "tripartite synapse," which proposes that glial cells are functional components of synapses (Araque et al., 1999).

In addition to intense and sustained network activity, neuronal communication also occurs at low rates at individual synapses. In fact, the release of neurotransmitters induced by single action potentials, known as basal synaptic transmission, is fundamental for information processing in the CNS. Astrocytes are ideally positioned to detect and modulate this type of activity because they extend processes that are in apposition with pre- and postsynaptic neuronal elements of synapses (Ventura and Harris, 1999; Witcher et al., 2007). It has been shown that astrocytes have intricate spongiform morphology with stubby main processes and dense ramifications with irregular shape (Bushong et al., 2002, 2004; Hama et al., 2004).

Despite this ideal position, the detection and modulation mechanisms in astrocytes are deemed too slow to be involved in local modulation of rapid, basal synaptic transmission. Indeed, although Ca^{2+} activities have been reported in glial processes (Nett et al., 2002; Perea and Araque, 2005; Santello et al., 2011; Wang et al., 2006), Ca^{2+} signaling has been generally studied globally in the whole astrocyte, where the slow timescale of Ca^{2+} changes precludes any spatial and temporal match with fast and localized synaptic transmission. Moreover, trains of sustained stimulation of afferents were necessary to induce this type of glial Ca^{2+} activity. Thus, it remains unknown whether astrocytes can detect single evoked synaptic events and respond by modulating basal transmission.

We addressed this issue by adapting for the study of neuron-glia interactions, imaging and electrophysiological techniques

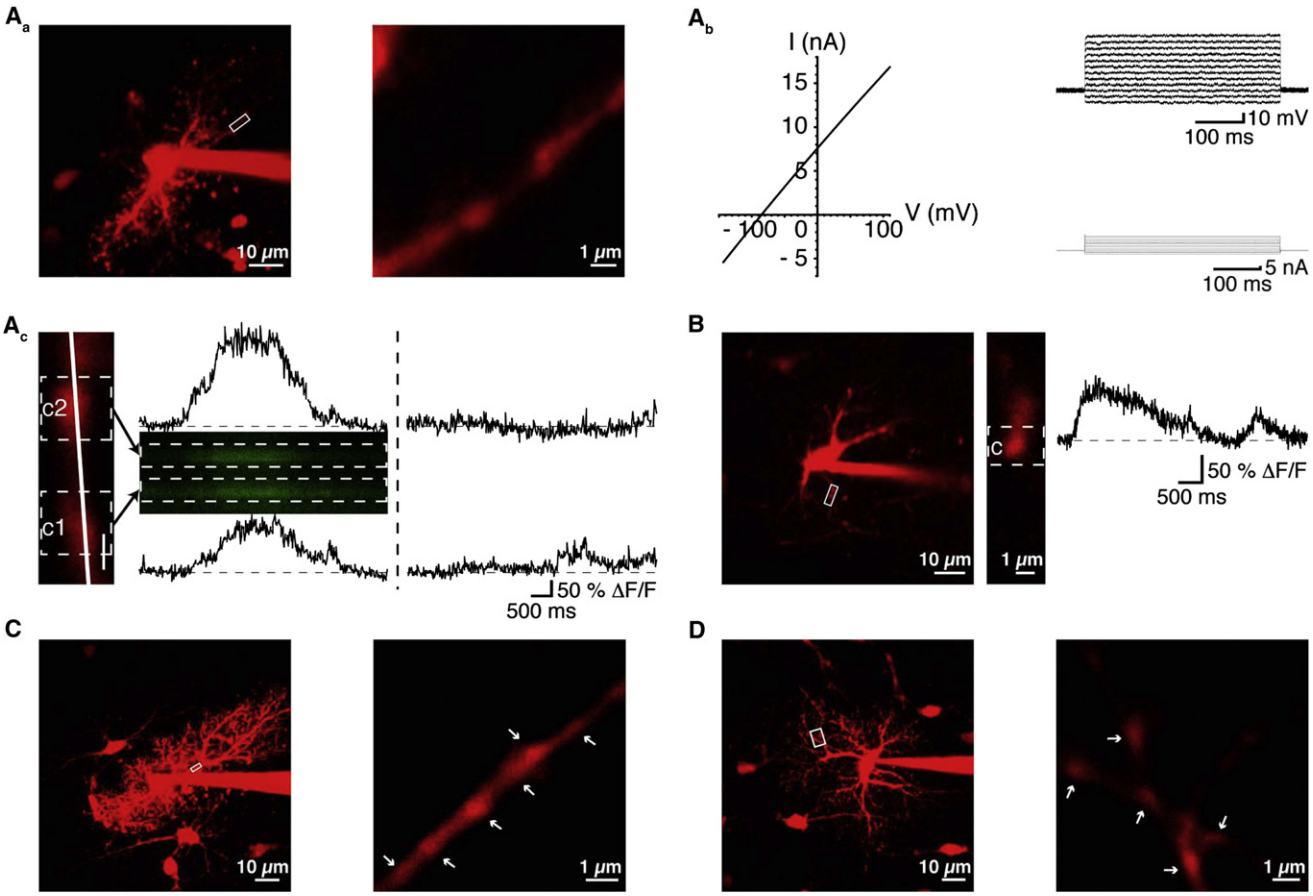

Figure 1. Spontaneous Ca^{2+} Activity Occurs Locally in the Astrocytic Process

(A) (Aa) Single-photon stack image of a recorded astrocyte in an acute hippocampal slice. (Right) Image of a process at higher magnification (white rectangle in left image). (Ab) This astrocyte was characterized by a linear current-voltage relationship in voltage-clamp configuration (left) and no action potential in current-clamp configuration (right). (Ac) Line-scan imaging of spontaneous Ca^{2+} events of the process presented in (Aa). The line on the process (left) indicates the position of the line-scan, and dotted lines show the boundaries of the regions of interest. Ca^{2+} events (traces, right) were observed in two compartments (c1 and c2).

(B) Example of a spontaneous Ca^{2+} event in a compartment from a different astrocyte.

(C and D) Two photon stack images of recorded astrocytes (left). Higher-magnification images (right, corresponding to boxed areas indicated in left images) show small broadenings along the main axis of astrocytic processes (arrowheads).

routinely used to study basal synaptic activity on dendritic spines. We show that astrocytes detect synaptic activity induced by single-synaptic stimulation in functional compartments along their processes. Following their activation via metabotropic glutamate subtype 5 receptors (mGluR5) during basal synaptic transmission, astrocytes increase the efficiency of transmission in CA1 pyramidal cells through activation of presynaptic adenosine A_{2A} receptors. These data suggest that astrocytes are directly involved with neurons in regulating elementary aspects of synaptic transmission.

RESULTS

Spontaneous Ca^{2+} Events Occur Locally along the Astrocytic Process

For astrocytes to participate in basal synaptic activity, a prerequisite is that Ca^{2+} signaling occurs locally along their processes. This was tested by monitoring spontaneous Ca^{2+} signals in astrocytes of CA1 stratum radiatum of acute hippocampal slices. Whole-cell patch-clamp recordings were performed to identify astrocytes and specifically introduce different compounds in these cells. All experiments were done on astrocytes (1) with a small cell body (diameter 8.3 ± 0.2 µm; n = 25 cells), (2) that are part of a network (neighboring somata in Figures 1Aa, 1C, and 1D), and (3) that have a low resting input resistance (14.7 ± 0.9 MΩ, n = 40 cells), a linear current-voltage relationship, and no action potential spiking behavior (Figure 1Ab). As reported previously (Bushong et al., 2002, 2004; Hama et al., 2004), we observed with confocal or two-photon microscopy that astrocytes loaded with Alexa Fluor 594 exhibited intricate spongiform morphology, dense process ramifications of irregular shape with frequent small broadenings (Figure 1). These enlargements (1.4 ± 0.04 µm; n = 136, 58 cells; Figure 1) measured along the main axis of the astrocytic process will be referred to as astrocytic compartments.

Characteristics of Ca^{2+} transients in these compartments were studied using fast confocal Ca^{2+} imaging in line-scan

mode along a small segment of an astrocytic process (5–20 μm; Figures 1A and 1B). Spontaneous Ca^{2+} responses were observed in compartments (Figures 1Ac and 1B) with an amplitude of ΔF/F = 92.2% ± 9.3% and a rise time of 277.7 ± 38.8 ms (n = 66 events in 35 compartments, 23 cells). These data are consistent with previous observations of spontaneous Ca^{2+} responses in astrocytic processes (Nett et al., 2002; Perea and Araque, 2005; Santello et al., 2011; Wang et al., 2006) and reveal the rapid kinetics of Ca^{2+} transients in small compartments along astrocytic processes.

Astrocytes Detect Synaptic Activity Evoked by Single-Synaptic Stimulation

We next tested whether local Ca^{2+} responses could be elicited in these compartments by synaptic activity evoked locally by single-synaptic stimulation. As shown in Figure 2A, single pulse stimulation of neuronal presynaptic elements evoked local Ca^{2+} events in an astrocytic process. Their amplitude was 128% ± 20.2% ΔF/F with a rise time of 217.5 ± 37.0 ms (n = 42 Ca^{2+} events in 14 compartments, 12 cells). The amplitude and rise time of evoked glial Ca^{2+} responses were not significantly different from the spontaneous ones (Mann Whitney test; $p > 0.05$). In addition, amplitude distribution of evoked glial Ca^{2+} responses was not different from that of spontaneous responses (chi-square test; $p = 0.17$; Figure 2B), suggesting that both populations of Ca^{2+} responses occur via similar mechanisms. To confirm the synaptic origin of evoked glial Ca^{2+} signals, we used tetrodotoxin (TTX) to prevent nerve-impulse propagation via the blockade of voltage-gated Na^+ channels. TTX (1 μM) completely blocked glial Ca^{2+} responses (Figure 2C; n = 5 compartments, 5 cells), indicating that they were not caused by direct stimulation of the astrocytic process or by mechanical perturbation.

Simultaneous recordings of astrocytes and pyramidal neurons were performed next to confirm that evoked Ca^{2+} responses in compartments of astrocytic processes correlated with basal synaptic activity. Minimal synaptic stimulation that activates putative single presynaptic fibers (Raastad et al., 1992) induced a rapid and local Ca^{2+} event in the glial compartment simultaneously with excitatory postsynaptic currents (EPSCs) (Figure 2D; n = 5 pairs). Interestingly, the absence of fluorescent changes outside of the boundaries of the compartment suggests that the Ca^{2+} event is compartmentalized. These results indicate that astrocytes detect small levels of neurotransmitter released locally, simultaneously with its detection by the postsynaptic neuron.

This conclusion was further supported when comparing the probabilistic nature of synaptically evoked local Ca^{2+} responses in astrocytes and EPSCs. Indeed, Ca^{2+} responses could be elicited repetitively in the same glial compartment, and similar to the synaptic currents, stimulation-evoked local glial Ca^{2+} responses showed failures (Figure 2E). The failure rate was 60.1% ± 8% for Ca^{2+} responses (n = 6) and 51% ± 6% for synaptic currents. Notably, Ca^{2+} response failure rate was never smaller than that of synaptic current. This is consistent with the nature of synaptic responses evoked by minimal stimulation whereby more than one synapse may be activated while only one glial compartment was studied. Furthermore, increasing the stimulus intensity decreased both the failure rate of synaptic currents and glial Ca^{2+} responses up to a point that failures were no longer observed. In these conditions, it was possible to evoke Ca^{2+} responses without failures with stimulation intervals of 30 s (data not shown).

Discrete Functional Organization along the Glial Process

The occurrence of local Ca^{2+} responses elicited by single synaptic stimulation implies that a discrete functional organization was present along the glial process.

First, we determined whether astrocytic compartments were in close morphological relationship with the postsynaptic site of glutamate synapses, dendritic spines (Ventura and Harris, 1999; Witcher et al., 2007). As shown in Figures 3A and 3B, small compartments of an astrocytic process identified after deconvolution and reconstruction were 1.5 ± 0.1 μm in length (n = 11 compartments of 5 astrocytes in 5 experiments). This is not statistically different from those observed with labeling experiments during whole-cell recording and Ca^{2+} imaging (Student's unpaired t test; $p > 0.05$). More importantly, these compartments were found in close apposition with dendritic spines. These results suggest that compartments along astrocytic processes that show local and discrete Ca^{2+} activity are associated with postsynaptic elements of glutamate synapses.

Second, we investigated whether glutamate receptors were functionally segregated along the astrocytic process. We tested whether release of glutamate at discrete locations along an astrocytic process elicited Ca^{2+} responses using local two-photon activation of the caged-glutamate compound MNI-glutamate (Carter and Sabatini, 2004; Smith et al., 2003). As predicted, photoactivation at specific and restricted areas adjacent to astrocytic compartments elicited Ca^{2+} responses at many locations (n = 19 evoked events on 36 trials onto 16 compartments, 9 cells; Figure 3C). Their amplitude was 84.9% ± 11.8% ΔF/F, with a rise time of 226 ms ± 52 ms, values that are not significantly different than those of spontaneous and synaptically evoked Ca^{2+} responses (one-way ANOVA, corrected with Dunn's multiple comparison test; $p > 0.05$). Furthermore, their amplitude distribution was similar to those of spontaneous and stimulation-evoked responses (Figure 3D; chi-square test, $p = 0.17$). This suggests that Ca^{2+} responses elicited by local photoactivation of MNI-glutamate are representative of those evoked by endogenous synaptic activity. These data indicate that functional glutamate receptors are segregated at discrete locations on compartments along astrocytic processes.

Astrocytes Modulate Basal Synaptic Transmission

We next tested whether astrocytes regulate the basal level of synaptic activity as a consequence of their detection of local neurotransmitter release. We used the Ca^{2+} chelator BAPTA to block selectively the rise of Ca^{2+} in astrocytes, a strategy that is known to prevent Ca^{2+}-dependent glial modulation of synaptic transmission (Serrano et al., 2006).

A pyramidal neuron was recorded in whole-cell configuration, and a neighboring astrocyte was contacted with a patch electrode containing BAPTA (10 mM) to form a cell-attached configuration, keeping the membrane intact to prevent BAPTA

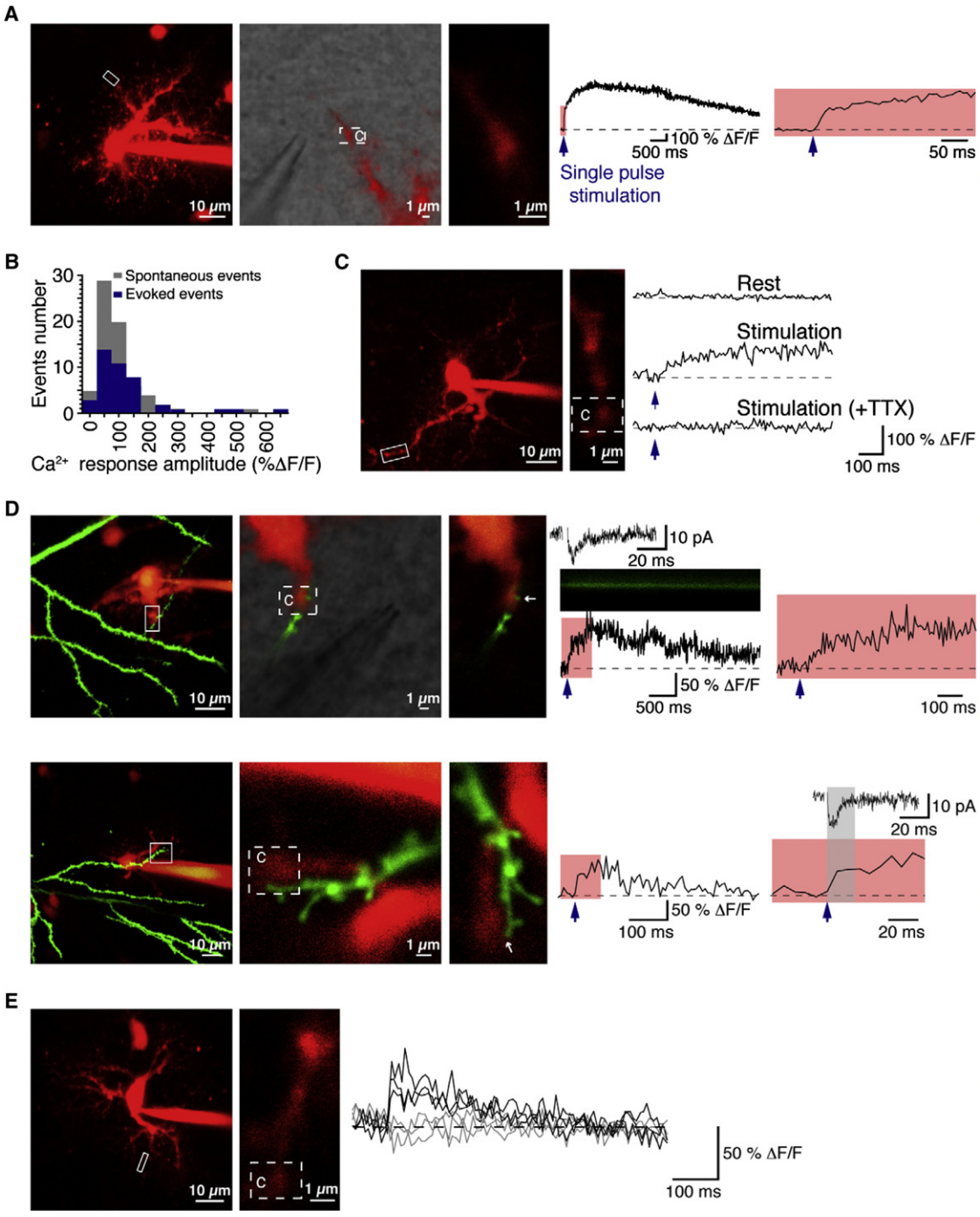

Figure 2. Astrocytes Detect Synaptic Activity Evoked by Single-Synaptic Stimulation

(A) Single-focal stimulation of Schaffer collaterals induced a Ca^{2+} response (right) at the level of the glial compartment identified along the astrocytic process (left).

(B) Amplitude distribution histogram (bin size, 25%ΔF/F) of spontaneous (gray) and evoked (blue) Ca^{2+} events recorded in astrocytic compartments. Evoked Ca^{2+} events appear as a subpopulation of the spontaneous Ca^{2+} events.

(C) TTX abolished Ca^{2+} responses evoked in a compartment of an astrocytic process.

(D) Two experiments (top and bottom) of paired recordings of an astrocyte (red) and a pyramidal neuron (green). A stimulating electrode was positioned near a glial compartment in interaction with the dendrite (top-middle image). (Right) Local glial Ca^{2+} responses (bottom traces) were evoked simultaneously with excitatory postsynaptic currents (top trace).

(E) Recorded astrocyte (left) and a process at higher magnification (white rectangle in left image). Repetitive Ca^{2+} responses (right traces) were elicited in the same compartment by single-fiber stimulation (black traces). Note the presence of failures (gray traces).

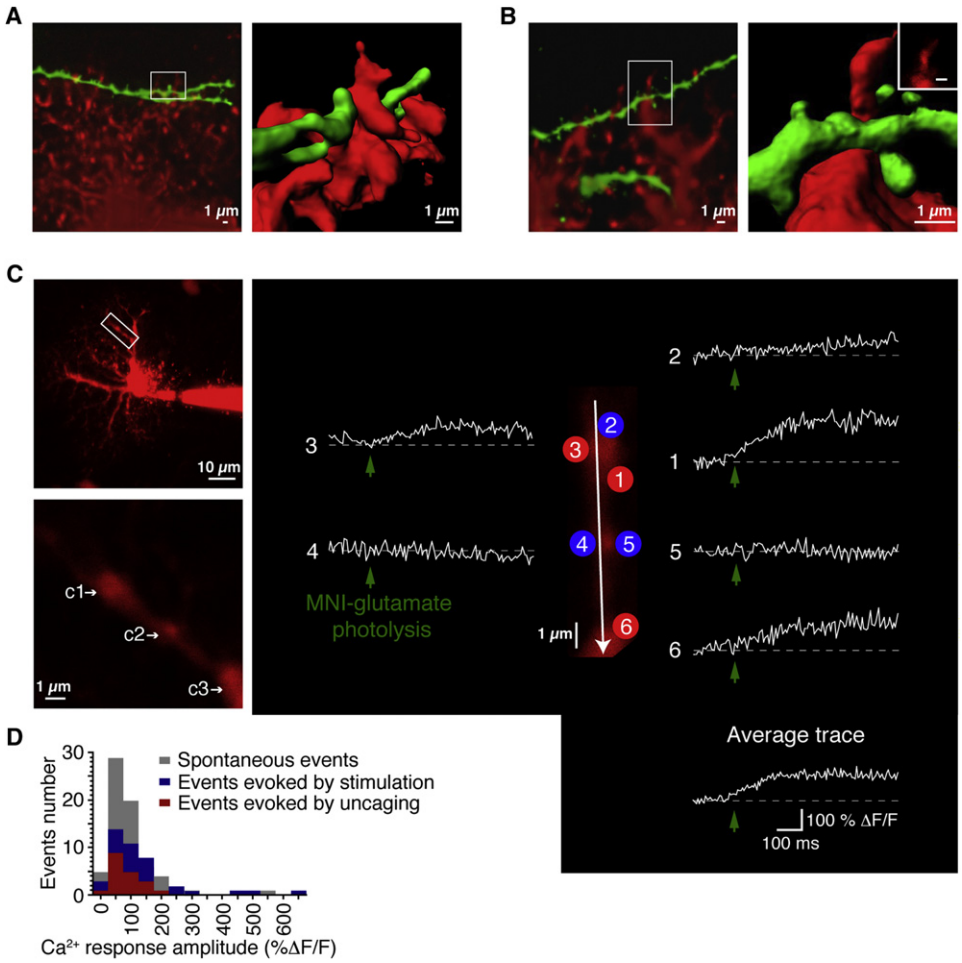

Figure 3. The Astrocytic Process Is Functionally Organized

(A and B) Stacks of confocal images of labeled astrocyte (red) and pyramidal neuron (green) after deconvolution (left). 3D reconstructions (right) of the indicated region (white rectangle in left images) show astrocytic compartments in close apposition with spines.

(C) Confocal stack image of a recorded astrocyte (upper-left) and three compartments imaged at higher magnification (c1, c2, and c3; lower-left). Local photoactivation of the glutamate-caged compound (MNI-glutamate, 10 mM) at specific areas of compartments 1 and 3 (red dots) elicited Ca^{2+} events in corresponding enlargements of the astrocytic process. The average Ca^{2+} response is shown on the lower-right.

(D) Histogram distribution of the amplitude of Ca^{2+} events evoked by MNI-glutamate uncaging (red), shown in comparison to spontaneous (gray) and stimulation-evoked (blue) Ca^{2+} events (bin size of 25%ΔF/F; same as Figure 2B for ease of comparison). Ca^{2+} events evoked by photoactivation of MNI-glutamate appear as a subpopulation of the others.

diffusion in the cell. EPSCs were evoked by minimal stimulation, and after 10 min of recordings of basal synaptic transmission, the membrane of the astrocyte was ruptured to establish whole-cell configuration and BAPTA diffusion into the astrocyte while EPSCs were continuously monitored up to 20 min after astrocyte break-in. The failure rate increased from 43.5% ± 2.2% in control to 91.1% ± 2.1% in BAPTA (Figures 4A and 4C; n = 6; Student's paired t test; $p < 0.05$), but the potency of responses (mean EPSC amplitude excluding failures) remained unchanged (−17.9 ± 2.1 pA in control and −13.0 ± 2.2 pA in BAPTA; Student's paired t test; $p > 0.05$), indicative of a presynaptic regulation of the efficacy of transmission. This effect cannot be due to the experimental procedure because experiments performed in the absence of the chelator in the patch electrode (Figures 4B and 4C) did not alter the failure rate (52.4% ± 13.1% in control to 48.8% ± 10.2% after break-in; $p > 0.05$) or the potency (−19.1 ± 1.0 pA in control and −21.5 ± 2.7 pA after break-in; $p > 0.05$). These results suggest that astrocytes regulate basal synaptic transmission in a Ca^{2+}-dependent manner by altering presynaptic activity.

We next tested whether subsequent stimuli are being influenced by prior activity. Monitoring changes in failure rate of synaptic responses elicited at 2 s and 10 s intervals revealed that it was unaltered throughout the recording period (Figure 4D). With an interval of 2 s, the initial failure rate went from 43.2% ± 5.6% to 47.8% ± 8.0% at the end of the 8 min recording period (one-way ANOVA with Tukey's multiple comparison test; $p > 0.05$; n = 6), whereas, at an interval of 10 s, the failure rate was 53.1% ± 6.1% initially and 57.3% ± 7.1% at the end of the recording period (one-way ANOVA with Tukey's multiple

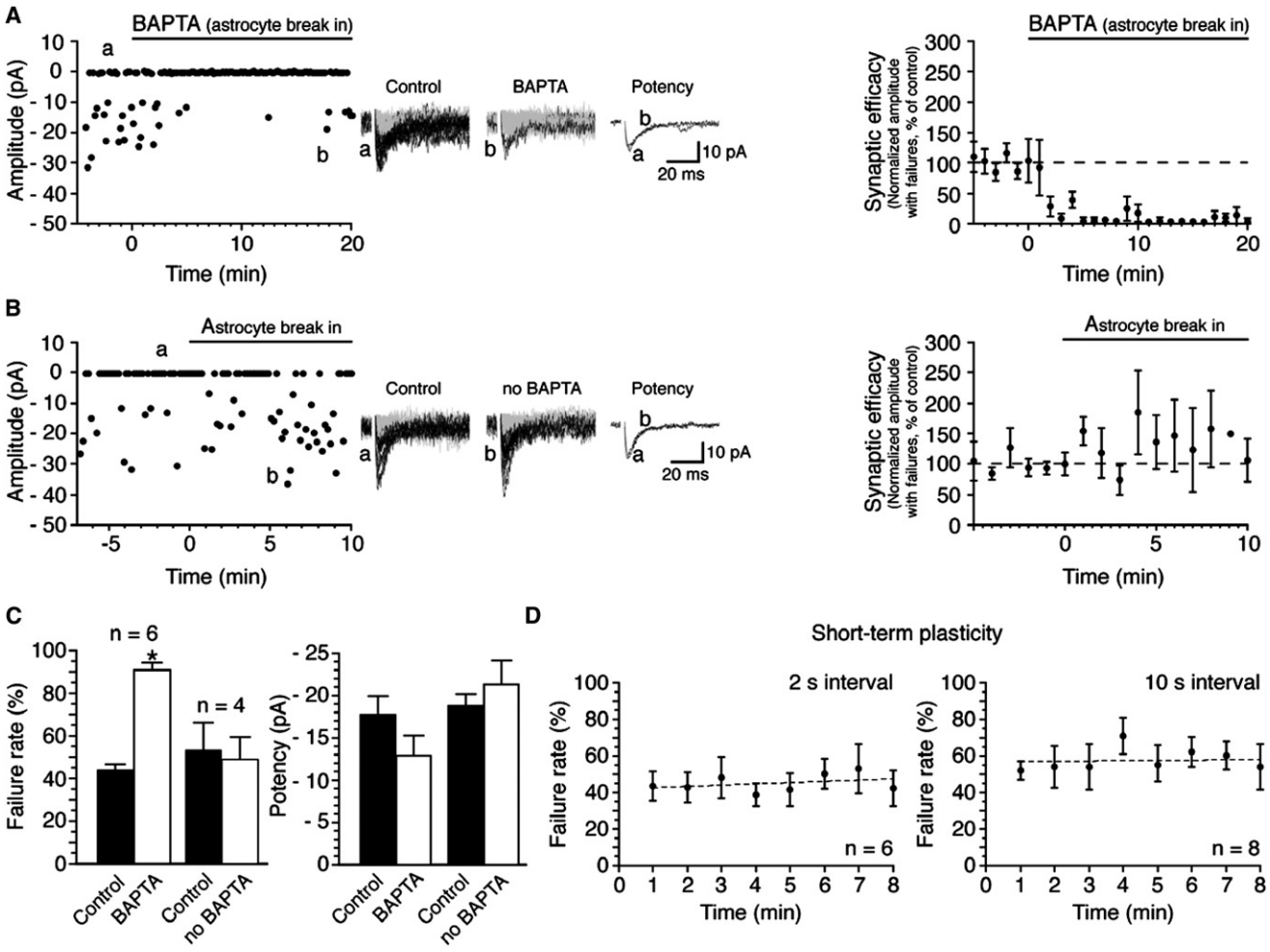

Figure 4. Astrocytes Regulate Basal Synaptic Transmission

(A) Plot of amplitude of responses evoked by minimal synaptic stimulation from a representative cell (left graph). Each point represents the peak amplitude of an individual event. Traces (middle) represent 20 superimposed successive events (EPSCs and failures) before (a, control) and after BAPTA dialysis (10 mM) in the recorded astrocyte (b, BAPTA). The two superimposed traces (a and b; right) correspond to EPSC potency in each condition (average EPSCs excluding failures). The time course for all cells is shown in the right panel. Each recording was binned and averaged in 1 min segments (including failures) and then normalized to the average EPSC amplitude recorded prior BAPTA dialysis in the astrocyte. These results reveal blockade of a presynaptic enhancement of basal transmission at individual synapses.

(B) Similar type of experiments showing no change in failure rate or potency when BAPTA was omitted from the patch electrode.

(C) Histograms summarizing the effect of BAPTA and control (no BAPTA) pipette solution on EPSC failure rate and potency. Data are reported as mean ± SEM. $^{*}p < 0.05$.

(D) Percentage of failure rates of synaptic responses evoked at intervals of 2 and 10 s. Each point represents the mean ± SEM of 30 trials at 2 s interval and 6 trials at an interval of 10 s. The failure rate did not change during the course of the experiment.

comparison test; $p > 0.05$; $n = 8$). This suggests that the glial modulation regulates basal synaptic transmission in a tonic fashion, independent of short-term plasticity.

mGluR5 Mediates Astrocyte Activation and Upregulation of Basal Synaptic Transmission

We next investigated the type of receptors involved in astrocyte activation by synaptic transmission. Group I metabotropic glutamatergic receptors, in particular mGluR5, are the major subgroup of receptors implicated in the detection of glutamate by astrocytes (Cai et al., 2000; D'Ascenzo et al., 2007; Fellin et al., 2004; Perea and Araque, 2005). Hence, we tested whether mGluR5 is implicated in the detection of the synaptic signal. Ca^{2+} responses were evoked by single-pulse stimulations in control conditions (Figure 5A; 232.2% ± 39.1% ΔF/F; n = 6 compartments, 6 cells) and in the presence of the mGluR5-selective antagonist 6-methyl-2-(phenylethynyl)-pyridine (MPEP, 25 μM). The presence of MPEP completely abolished local Ca^{2+} events (Figure 5A; n = 6 compartments, 6 cells). In two of these experiments, the recordings were kept long enough to wash out MPEP and obtain a recovery of evoked Ca^{2+} responses (Figure 5A; 198.9% ± 36.9% ΔF/F; n = 2 compartments, 2 cells). These results indicate

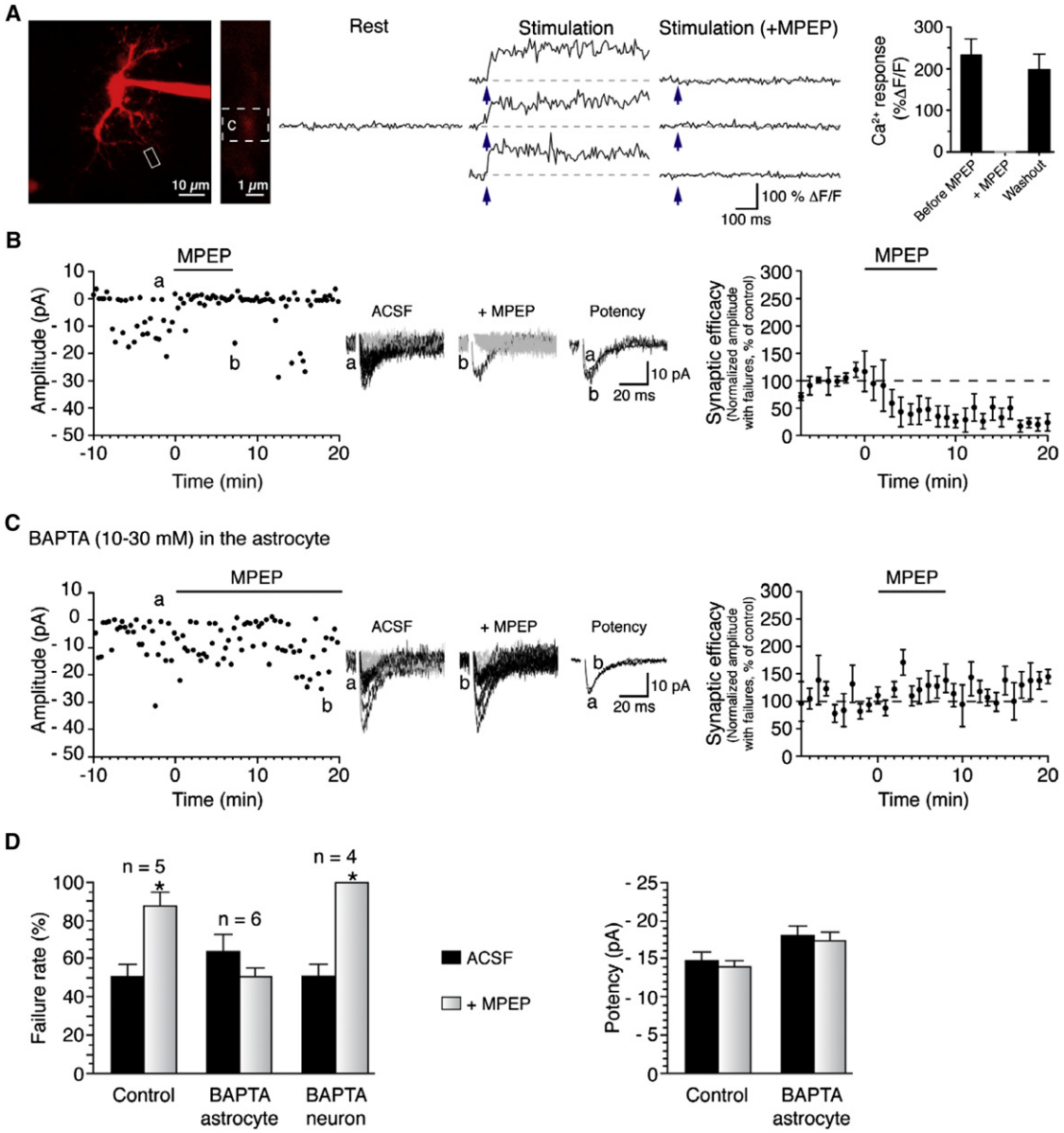

Figure 5. mGluR5-Dependent Endogenous Enhancement of Basal Transmission by Astrocytes

(A) Stimulation-induced Ca^{2+} responses in an astrocytic compartment were blocked by the antagonist of mGluR5, MPEP (25 μM). The histogram on the right shows that this effect was reversible upon washout of the antagonist. Data are reported as mean ± SEM.

(B) Inhibition of mGluR5 receptors by MPEP (25 μM) increased EPSC failure rate but did not change potency.

(C) Similar experimental paradigm with intracellular dialysis with BAPTA (10 mM) in the astrocyte. In this condition, MPEP failed to affect basal transmission.

(D) Histograms summarizing the effect of MPEP (25 μM) on EPSC failure rate and potency and the block by BAPTA injection in the astrocyte. Data are reported as mean ± SEM. *$p < 0.05$. Artificial cerebrospinal fluid (ACSF).

that local Ca^{2+} responses elicited in compartments of astrocytic processes by single synaptic stimulation are mediated by activation of mGluR5.

A prerequisite for astrocytes to modulate basal synaptic transmission is that interfering with mGluR5 function should alter basal synaptic transmission in pyramidal cells, as did the injection of BAPTA in astrocytes. EPSCs evoked using minimal stimulation of putative single presynaptic fibers were recorded for 10 min in control ACSF solution and then in the presence of MPEP (25 μM). We found that the failure rate increased from 50.9% ± 6.1% in control to 87.9% ± 6.7% in MPEP (n = 5 cells; Student's paired t test; $p < 0.05$; Figures 5B and 5D), whereas the potency of synaptic currents was unchanged (−14.8 ± 1.1 pA in control, −13.9 ± 0.9 pA in MPEP; n = 5 cells; Student's paired t test; $p > 0.05$; Figures 5B and 5D). This indicates that mGluR5 activation upregulates

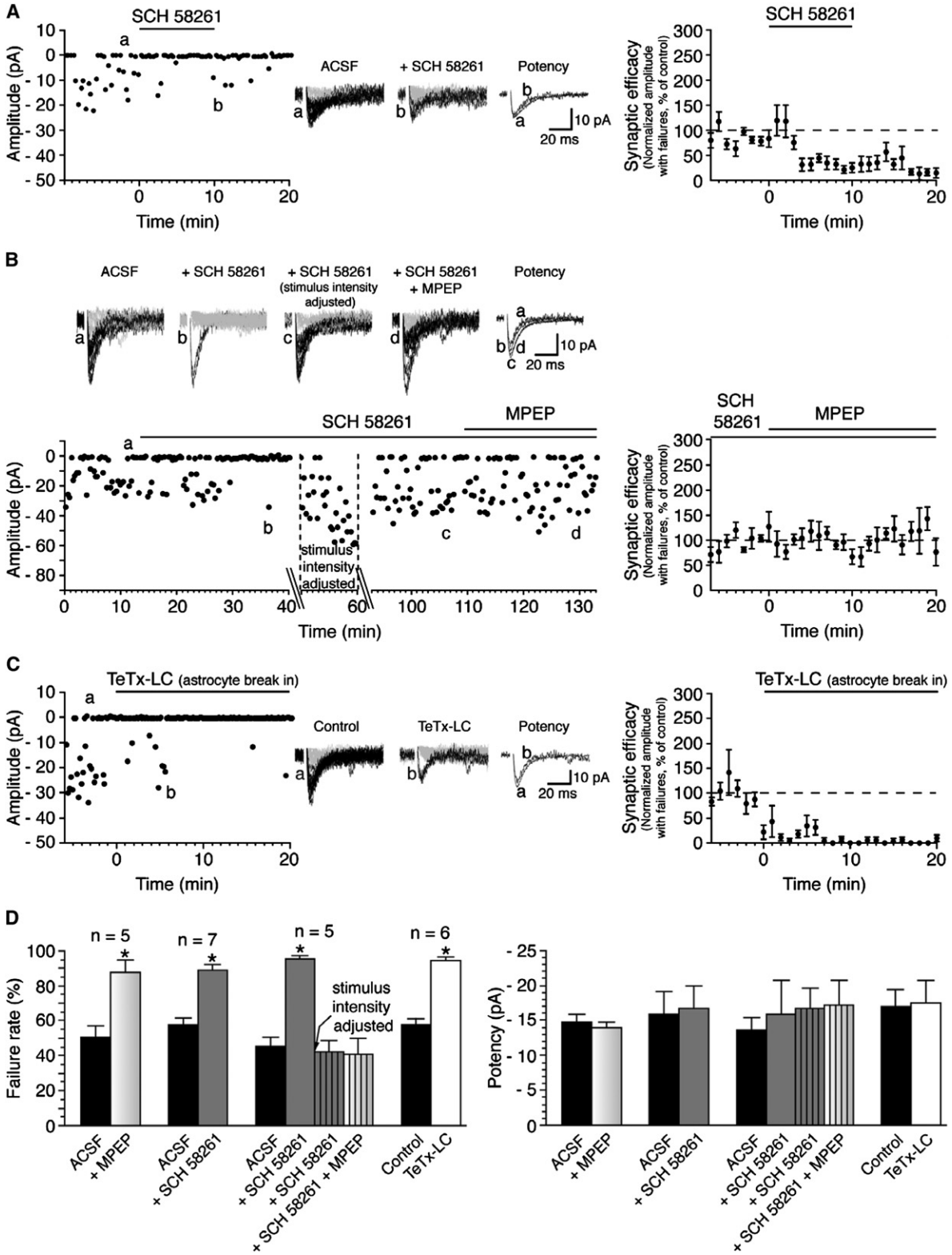

Figure 6. Astrocytes Increase Basal Synaptic Transmission through Presynaptic A_{2A} Receptor Activation

(A) Inhibition of A_{2A} receptors by SCH 58261 (100 nM) increased EPSC failure rate.

(B) Once A_{2A} receptors were inhibited, MPEP failed to impair minimal synaptic transmission. This suggests that A_{2A} receptors were activated downstream of mGluR5.

the efficiency of basal transmission at individual pyramidal cell synapses.

Astrocytes Mediate the mGluR5-Dependent Increase in Basal Synaptic Transmission

Because basal synaptic transmission activates astrocytes in a Ca^{2+}- and mGluR5-dependent manner and buffering Ca^{2+} in astrocytes and mGluR5 antagonism impaired basal synaptic transmission, we next assessed whether astrocytes are involved in the mGluR5-mediated modulation of basal synaptic transmission. One would predict that the MPEP effect on basal synaptic transmission should be masked by selective blockade of Ca^{2+} signaling in astrocytes.

Intracellular dialysis of BAPTA (10–30 mM) in an astrocyte prevented completely the increase in failure rate of EPSCs that was normally induced by MPEP (Figures 5C and 5D; from 63.3% ± 9.1% in control to 50.8% ± 4.6% in MPEP; n = 6 experiments; Student's paired t test; $p > 0.05$). Synaptic potency remained unchanged (−18.1 ± 1.2 pA in control, −17.4 ± 1.1 pA in MPEP; n = 6 experiments; Student's paired t test; $p > 0.05$). These results suggest that Ca^{2+}-dependent astrocyte activity is necessary for the mGluR5-dependent regulation of basal synaptic transmission.

Another possibility is that MPEP effects on basal synaptic transmission were due to mGluR5-mediated Ca^{2+} signaling in pyramidal neurons (Holbro et al., 2009). This was tested by intracellular perfusion of BAPTA in the postsynaptic pyramidal neuron and examining MPEP effects on minimally evoked EPSCs. Injection of BAPTA (20 mM) in pyramidal neurons did not impair MPEP effects, as the EPSC failure rate increased from 50.0% ± 6.7% in control to 100% with MPEP (n = 5 cells; Student's paired t test; $p < 0.05$; Figure 5D). Hence, it is unlikely that the MPEP effect occurs through its action on mGluR5 in pyramidal cells. It is also unlikely that the effect could be mediated by a presynaptic action of glutamate, as the known presynaptic glutamatergic receptors are negatively linked to transmitter release (Ayala et al., 2008).

Together, our observations show that Ca^{2+} responses are evoked by single-synaptic stimulation in astrocytic processes via mGluR5 and that interfering specifically with astrocyte Ca^{2+} signaling impairs the mGluR5-mediated regulation of basal transmission. Importantly, spontaneous intrinsic Ca^{2+} events in astrocytes are unlikely to mediate this effect because they are mGluR independent (Nett et al., 2002). This reveals that mGluR5-mediated activation of astrocytes enhances basal synaptic transmission in pyramidal neurons.

Astrocytes Increase Basal Synaptic Transmission through Presynaptic A_{2A} Receptor Activation

An intermediary step involving the release of a gliotransmitter is required in this synaptic modulation because our data indicate that astrocytes activation is necessary for the subsequent presynaptic potentiation. We considered the possible role of adenosine because purines are well-known gliotransmitters (Halassa and Haydon, 2010; Volterra and Meldolesi, 2005), and adenosine (via A_{2A} receptor activation) facilitates transmitter release at hippocampal glutamatergic synapses (Cunha, 2001).

A first prerequisite is that inhibition of presynaptic A_{2A} receptors mimics the effect of mGluR5 antagonist. Inhibition of A_{2A} receptors by SCH 58261 (100 nM) increased EPSC failure rate from 58.1% ± 3.7% in control to 88.7% ± 3.5% in SCH 58261 (Figures 6A and 6D; n = 7 cells; Student's paired t test; $p = 0.0001$), whereas the potency was unaltered (−15.8 ± 3.3 pA in control, −16.8 ± 3.2 in SCH-58261; n = 7 cells; Student's paired t test; $p > 0.05$). Importantly, this effect was not statistically different than the effect induced by MPEP ($p > 0.05$).

Our working model suggests that adenosine A_{2A} receptors should be recruited downstream of the mGluR5-mediated glial activation. Hence, the effect of MPEP on synaptic transmission should be occluded following A_{2A} receptor blockade. Experiments above were repeated, and blockade of A_{2A} receptors by SCH 58261 increased EPSC failure rate (45.5% ± 4.9% in control, 95.5 ± 1.7% in SCH-58261; n = 5 cells; Student's paired t test; $p < 0.01$; Figures 6B and 6D) with no effect on potency (−13.6 ± 1.7 pA in control, −15.8 ± 4.9 pA in SCH-58261; n = 5 cells; Student's paired t test; $p > 0.05$). Stimulus intensity was then adjusted in the presence of SCH 58261 to restore EPSC failure rate to ~50%, and MPEP was subsequently applied. As shown in Figures 6B and 6D, EPSC failure rate was not altered by MPEP following initial blockade of A_{2A} receptors (42% ± 6.7% in SCH 58261 and 41% ± 9.1% in MPEP in the presence of SCH 58261; n = 5 cells; Student's paired t test; $p > 0.05$), and the potency remained unchanged (−16.8 ± 2.8 pA in SCH 58261, −17.2 ± 3.6 pA in MPEP and SCH 58261; n = 5 cells; Student's paired t test; $p > 0.05$).

Because the release of purines by astrocytes is known to be dependent on tetanus toxin-sensitive protein interactions (Pascual et al., 2005), the contribution of purines that are released by astrocytes was further substantiated by testing the effect of the light chain of tetanus toxin (TeTx-LC) on basal synaptic transmission. Using the same approach of BAPTA dialysis into astrocytes (Figure 4), we found that the diffusion of TeTx-LC (1 μM) in astrocytes increased the failure rate of synaptic currents evoked by minimal stimulation (58.4% ± 3.0% in control, 95.3% ± 1.8% in TeTx-LC; Figures 6C and 6D; n = 6; Student's paired t test; $p < 0.05$), whereas the potency was unaltered (−17.3 pA ± 2.4 pA in control, −17.7 pA ± 3.2 pA after TeTx-LC; n = 6, Student's paired t test; $p > 0.05$). These data are consistent with the notion that purines released by astrocytes regulate basal synaptic transmission.

These results indicate that the mGluR5-dependent enhancement of basal synaptic transmission involves the downstream activation of presynaptic A_{2A} receptors by astrocyte-derived purines.

Differential Distribution of mGluR5 and A_{2A} Receptors

Our data suggest that mGluR5 should be present on astrocyte processes, whereas A_{2A} receptors should be found in presynaptic

(C) Dialysis of the TeTx-LC (1 μM) in an astrocyte increased the failure rate of EPSCs without altering the potency.
(D) Histograms summarizing the effects of MPEP, SCH 58261, and TeTx-LC on failure rate and potency. For ease of comparison, data summarizing the effect of MPEP (same data as Figure 4D) are also reported. Arrow indicates adjustment of stimulation intensity. Data are reported as mean ± SEM. *$p < 0.05$.

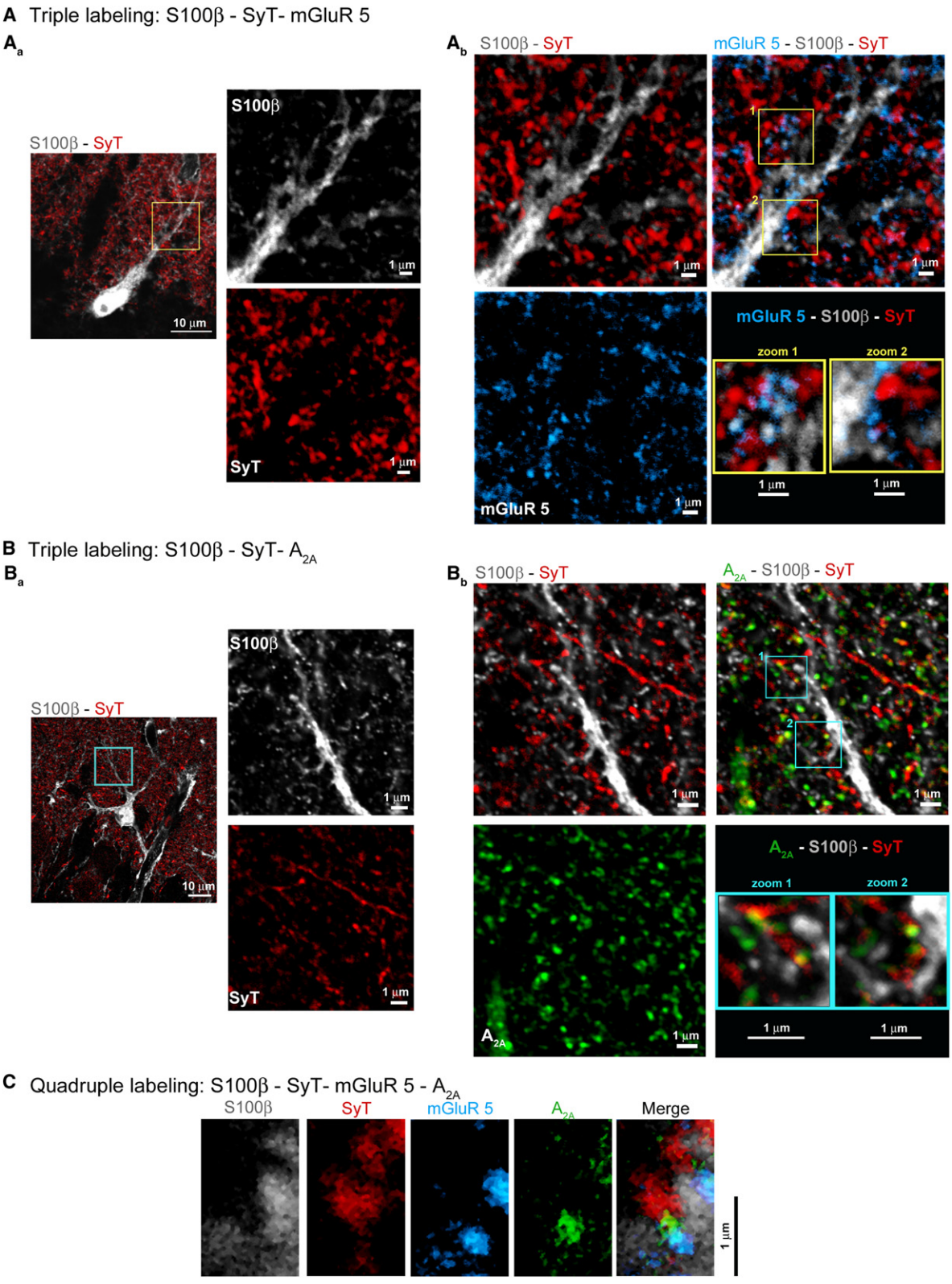

Figure 7. Differential Distribution of mGluR5 and A_{2A} Receptors

(A) False color confocal images of immunolabeling of S100β (gray) in astrocytes, of synaptotagmin (SyT, red) in presynaptic terminals, and mGluR5 (cyan) acquired simultaneously. (Aa) Images at low (left) and high magnification (corresponding box in left image). (Ab) High magnification of S100β and synaptotagmin

terminals. We performed immunohistochemical staining to examine the relative distribution of these receptors, using S100β as an astrocyte marker and the vesicular protein synaptotagmin as a presynaptic marker.

Both labelings showed characteristics expected from glial and presynaptic markers (Figures 7Aa and 7Ba). For S100β labeling, detailed arborisation of glial cells, astrocytes in particular, was routinely observed (n = 5 animals, 49 sections). Astrocytes were identified as cells with extensive ramifications and a process associated with a blood vessel (Bushong et al., 2002). These cells had several primary, secondary, and tertiary processes and a detailed morphological organization that is consistent with astrocytes (Matthias et al., 2003). We observed enlargements along the processes of S100β-labeled astrocytes of similar size and shape as those observed with intracellular labeling with fluorescent markers. The synaptotagmin labeling was punctate, consistent with its presence in synaptic boutons (Tartaglia et al., 2001). Importantly, although synaptotagmin puncta were occasionally observed in astrocytes, consistent with the role of this protein in astrocytes (Zhang et al., 2004), S100β and synaptotagmin labeling seldom overlapped, indicating that they were selective glial and presynaptic markers.

The mGluR5 labeling was punctated, with puncta present along S100β-positive glial processes (Figure 7Ab; n = 6 animals, 29 sections). Importantly, mGluR5 puncta were often found on small enlargements along S100β-positive astrocytic processes, facing a synaptotagmin-positive presynaptic element. Puncta of mGluR5 were also observed independent of glial labeling and often juxtaposed to synaptotagmin puncta, consistent with the perisynaptic location of these receptors in pyramidal cells (Lujan et al., 1996).

A_{2A} receptor labeling was also punctated, but the puncta were almost never seen on S100β-positive glial processes (Figure 7Bb). In fact, S100β and A_{2A} labeling were almost entirely exclusive (n = 3 animals, 18 sections). However, consistent with our physiological data and the presence of these receptors on presynaptic terminals (Rebola et al., 2005), the A_{2A} labeling was often colocalized with the synaptotagmin-positive presynaptic elements (Figure 7Bb). Doublets of A_{2A} receptor and synaptotagmin puncta were often seen facing a compartment of an S100β-positive glial process. Finally, quadruple immunolabeling revealed that mGluR5 puncta on S100β-positive glial processes were juxtaposed to A_{2A} receptor- and synaptotagmin-positive presynaptic elements (n = 1 animal, 10 sections; Figure 7C).

This relative distribution of receptors is fully consistent with the mGluR5-dependent detection of basal synaptic transmission by astrocytes, their ability to release purines in a TeTx-dependent manner, and the regulation of Schaffer collateral synapses via presynaptic A_{2A} receptors.

DISCUSSION

Our results indicate that astrocytes, like neurons, perform local processing of synaptic information at the level of individual synapses. Astrocytes of the hippocampal CA1 region detect synaptic activity and upregulate basal synaptic transmission. These findings uncover a major conceptual advance in our understanding of brain communication, as elementary synaptic communication at central synapses is not solely neuronal in nature but is subject to endogenous regulation by astrocytes.

Functional Compartments along Processes of Astrocytes

Our observations are consistent with findings that Ca^{2+} responses can be evoked in distinct areas of Bergmann glial cells (Grosche et al., 1999). However, they used supramaximal axonal stimulation rather than the minimal synaptic stimulation used here. Rapid detection of glutamatergic transmission by astrocytes occurs also via glutamate transporter currents generated by synaptic release of glutamate (Bergles and Jahr, 1997). Although this is an important regulator of synaptic activity, synaptic modulation by astrocytes in the hippocampus is driven by receptor activation and Ca^{2+}-dependent mechanisms. Hence, the ability of astrocytes to detect local basal synaptic activity reveals a level of glial sensitivity to neurotransmitters never reported before.

The rapid detection of synaptic events by astrocytes occurs at discrete subcellular functional sites that we identified as astrocytic compartments. Astrocytes may detect local vesicular release of neurotransmitter both at synaptic and ectopic sites (Matsui and Jahr, 2003). This is an intriguing possibility because ectopic transmitter release may act preferentially on the glial compartment, providing a privileged interaction between presynaptic terminal and astrocyte. Also, ectopic vesicular release is regulated differently than synaptic release (Matsui and Jahr, 2004), offering another level of modulation of transmitter release by astrocytes.

It has been reported that astrocytes interact with and detect activity at diverse types of synapses (Araque et al., 2002; Kang et al., 1998; Perea and Araque, 2005). For instance, astrocytes in stratum oriens of the hippocampal CA1 area detect synaptic activity induced by trains of stimuli to Schaffer collateral or alveus pathways (Perea and Araque, 2005) through different types of receptors and at distinct levels of glial processes. This suggests that astrocyte receptors are not localized arbitrarily but are compartmentalized at the level of synapses. This is consistent with mGluR5 immunostaining in the form of puncta along astrocyte processes. It would be interesting to determine whether specialized functional astrocyte compartments are associated with other types of synapses. In fact, there may be

(upper-left) shows the exclusion of the presynaptic marker from the glial process. Labeling of mGluR5 (lower-left) and the combination of the triple labeling (upper-right) illustrate the mGluR5 colocalization with S100β. Higher magnification of two regions is shown (lower-right). mGluR5 labeling decorates the astrocytic process, often facing a presynaptic puncta.

(B) Same organization as in A but for immunolabeling of A_{2A} receptors (green). Consistent with a presynaptic localization, the puncta of A_{2A} receptors were not present on glial processes but were often juxtaposed with a synaptotagmin puncta.

(C) False color confocal imaging at a high magnification of quadruple immunolabeling showing a portion of a S100β-positive astrocyte process (gray), synaptotagmin-positive presynaptic elements (SyT, red), mGluR5 (cyan), and A_{2A} receptors (green), as well as the merge image with all four labels. mGluR5 puncta was on a S100β-positive glial process, facing A_{2A} receptor juxtaposed to synaptotagmin-positive presynaptic elements.

other glial compartments in addition to those described. Indeed, sheet-like structures of smaller size have been reported (Hama et al., 2004) but would be below the spatial resolution of the imaging technique used here.

Finally, the detection of a high level of glutamate by astrocytes (Matsui and Jahr, 2003) and the probabilistic nature of the local Ca^{2+} responses reported here raise the possibility that astrocytes act like postsynaptic cells rather than a third synaptic partner. Interestingly, the correlation between the failure rate of Ca^{2+} responses in astrocyte compartments and synaptic currents in neurons is similar to the one between failure rates of Ca^{2+} responses in dendritic spines and synaptic responses of pyramidal cells (Reid et al., 2001).

Integrated Presynaptic and Glial Mechanisms

The regulatory role of astrocytes in basal synaptic transmission may be relevant to many other types of synapses in the CNS because they regulate synaptic transmission and plasticity in numerous brain areas (Gordon et al., 2009; Gourine et al., 2010; Matsui and Jahr, 2004; Matsui et al., 2005; Panatier et al., 2006). Hence, it is appealing to propose that a similar regulation may also be at play at other CNS synapses.

This glial modulation may serve to adjust synaptic efficacy so that it can be modulated according to various plasticity events taking place in the hippocampus. This balanced modulation requires that astrocytes can increase and decrease basal synaptic transmission. Interestingly, astrocytes can decrease transmitter release by activating presynaptic A_1 adenosine receptors (Pascual et al., 2005; Serrano et al., 2006; Todd et al., 2010), and during basal transmission, A_1 and A_{2A} receptors are activated, as we observed that an A_1 receptor antagonist (PSB-36) altered basal synaptic activity (data not shown). Also, glial cells at the neuromuscular junction use a balanced A_1-A_{2A} receptor modulation to differentially influence synaptic plasticity (Todd et al., 2010). Interestingly, their relative influence may be age dependent (Diógenes et al., 2007).

The regulation of basal synaptic transmission may allow astrocytes to integrate and adapt synaptic strength according to the history of the synapse. For instance, presynaptic upregulation of basal synaptic transmission that we uncovered may vary with long-term changes in synaptic efficacy such as long-term potentiation. This may even imply that astrocytes themselves undergo synaptic plasticity changes, as was recently shown for another type of perisynaptic glial cell (Bélair et al., 2010).

From Local Modulation to Global Integration

It is likely that, depending on the coincidence, pattern, and level of synaptic activity, the local modulation may be extended to the whole astrocyte by the propagation of the Ca^{2+} signals along astrocytic processes. An additional step would be to determine whether the resulting propagating signal has consequences on the efficacy of transmission of neighboring synapses. Interestingly, Perea and Araque (2005) reported that glutamatergic and cholinergic pathways in the CA1 region of hippocampus could influence each other and modulate the amplitude of the astrocytic Ca^{2+} signal and its propagation from processes to the soma. In this case, an astrocyte would then switch from a local integration process to a more global one and, hence, act as a synaptic network integrator. This implies that different sets of mechanisms and Ca^{2+} sensitivity must be involved. Consistent with this possibility, BAPTA in astrocytes did not alter the production of LTP at CA3-CA1 synapses, whereas a Ca^{2+} clamping solution prevented it (Henneberger et al., 2010). This suggests that the pattern, temporal profile, and magnitude of Ca^{2+} changes are critical for the astrocyte to perform different regulatory functions. However, one cannot easily predict the outcome of Ca^{2+}-dependent mechanisms based on the kinetics of Ca^{2+} responses obtained using mobile Ca^{2+} buffers because they greatly extend in time and space the magnitude of Ca^{2+} diffusion.

The different functions of astrocytes could be influenced by the types of receptors activated. For instance, we found that local Ca^{2+} responses are mediated by mGluR5, whereas other types of glutamatergic receptors (mGluR and NMDA receptors) are involved in other forms of astrocyte excitability and modulation (Halassa and Haydon, 2010). One may even consider that different types of receptors have distinct spatial organization along astrocytic processes in relation with various synaptic elements.

Integration of Information

The detection of local and rapid basal synaptic transmission by astrocytes strongly suggests that they discriminate multiple levels of communication, from basal synaptic activity at unitary synapses up to complex patterns of plurisynaptic network interactions (Fellin et al., 2004; Henneberger et al., 2010; Pasti et al., 1997; Perea and Araque, 2005; Porter and McCarthy, 1996; Serrano et al., 2006). Thus, astrocytes can specifically decode the pattern of synaptic activity and, in turn, modulate differentially the output of synaptic transmission. This is supported by the observation that specific patterns of glial Ca^{2+} activities induced distinct forms of synaptic plasticity at the neuromuscular junction (Todd et al., 2010).

Astrocytes use various mechanisms to achieve the different modulations by releasing distinct gliotransmitters. For instance, we showed that purines locally modulate basal synaptic transmission, whereas others showed that D-serine, purines, and glutamate were necessary for different forms of plasticity (Henneberger et al., 2010; Yang et al., 2003; Pascual et al., 2005; Serrano et al., 2006; Perea and Araque, 2007). Because astrocytes occupy exclusive domains within which they interact with several types of synapses (Bushong et al., 2002; Halassa et al., 2007), it is likely that they interact with and differentially modulate many synapses according to specific conditions driven by the various types of synapses.

In conclusion, astrocytes regulate synaptic information at many levels, including activity of single synapses. Recognition of this concept fundamentally changes our understanding of brain communication and the role of glial cells in synaptic function.

EXPERIMENTAL PROCEDURES

Slice Preparation

Transverse hippocampal slices (300 μm) were prepared from 15- to 21-day-old Sprague Dawley male rats (Charles River, Montréal, Québec, Canada) as described previously (Serrano et al., 2006). All experiments were performed in accordance with guidelines for maintenance and care of animals of the Canadian Council of Animal Care and Université de Montréal.

Electrophysiology

CA1 pyramidal neurons and astrocytes in stratum radiatum were identified using an infrared camera. Astrocytes were identified based on soma size ($\leq$10 μm), shape, and biophysical properties analyzed using whole-cell recordings as detailed in the Extended Experimental Procedures available online. Neurons and astrocytes were loaded with fluorescent marker via the patch electrodes for morphological analysis.

Synaptic Stimulations and Recordings

A stimulating glass microelectrode (3–5 MΩ) filled with ACSF was positioned using visual guidance in the vicinity (5–15 μm) of a fluorescently labeled astrocytic process (Goldberg et al., 2003; Yuste and Denk, 1995). Focal stimulations of Schaffer collaterals were evoked by single-pulse stimulation (0.2 ms, 7–40 μA) at a frequency of 0.033 Hz. Minimal synaptic stimulations of putative single-fiber (0.2 ms, 7–20 μA) (Raastad et al., 1992) were performed at 0.05, 0.1, or 0.5 Hz (details in Extended Experimental Procedures).

Live Morphological and Ca^{2+} Imaging

Ca^{2+} imaging was performed using the line-scan mode (500 Hz, 2 ms per line) and the 488 nm line of an Argon ion laser. Changes in fluorescence (ΔF) were measured as relative elevation from baseline fluorescence and expressed as % $\Delta F/F = [(F_{post} - F_{rest})/F_{rest}] \times 100$. Images were further analyzed off-line with LSM 510 (Carl Zeiss) and ImageJ (NIH) software (see Extended Experimental Procedures).

Two-Photon Uncaging of MNI-Glutamate

Uncaging of MNI-glutamate was performed with a mode-locked Ti:Saphire laser (Mira 900) operated at 720 nm wavelength (76 MHz pulse repeat, < 200 fs pulse width) pumped by a solid-state source (5 W Verdi argon ion laser; Coherent Santa Clara, CA). MNI-glutamate was applied in the bath (5 mM) or locally (10 mM; 10 psi; 1 min) using a glass electrode (3–5 MΩ) positioned at the surface of the slice above the recorded astrocyte. An uncaging spot on an astrocytic compartment (<0.8 micron away) was determined from a confocal image acquired using a HeNe 543 laser. Uncaging was induced for a single period of 2 ms exposure at 720 nm while performing line-scan imaging (500 Hz line/scan at 0.033 Hz).

Three-Dimensional Reconstructions

Confocal Z stack images (optical sections at 0.5 μm intervals) acquired from acute slices were deconvolved in three dimensions using Autodeblur software (Auto-Quant, Media Cybernetics, Silver Spring, MD). Deconvolved confocal Z stacks were rendered in three dimensions using IMARIS 6.2.0 (Bitplane, Zurich, Switzerland) as previously described (Haber et al., 2006).

Immunohistochemical Labeling and Image Acquisition

Hippocampal slices were prepared as above and sectioned (60 μm thick) using a sliding microtome (LEICA SM2000R). Sections were permeabilized for 30 min in a 0.3% Triton X-100 in PBS solution and then rinsed with a PBS/0.01% Triton X-100. Nonspecific labeling was blocked using 10% normal donkey serum (NDS). All primary and secondary antibody incubations were done in PBS/0.01% triton-100/2% NDS solution.

Two sets of triple labeling and one set of quadruple immunolabeling experiments were performed to examine the relative distribution of mGluR5 and A_{2A} receptors. Each receptor labeling was compared to a presynaptic marker using an antibody against the vesicular protein Synaptotagmin and to a glial marker using an antibody against the protein S-100β (see Extended Experimental Procedures).

Observations were done using an Olympus FV1000 scanning confocal microscope equipped with a 60× oil-immersion objective (N.A. 1.4). Images were acquired at a resolution of 512 pixels × 512 pixels with a dwell time of 8 μs per pixel (see Extended Experimental Procedures for details).

Statistical Analysis

Data were analyzed to determine whether they fitted a Gaussian population. Accordingly, a parametric or a nonparametric test was performed. The statistical differences were established at $p < 0.05$. Graphpad Prism software was used for statistical analysis. Data were expressed as mean ± SEM.

SUPPLEMENTAL INFORMATION

Supplemental Information includes Extended Experimental Procedures and can be found with this article online at doi:10.1016/j.cell.2011.07.022.

ACKNOWLEDGMENTS

We thank Dr. A. Serrano for helpful discussions and suggestions; Dr. J. Boehm for helpful comments on different versions of the manuscript; and Dr. K.M. Harris for her comments, discussion and for reading different versions of the manuscript. We also thank Ms. Pierrette Fournel for her technical support. This work was supported by grants from NSERC Discovery Group; by an infrastructure grant from FRSQ (Groupe de recherche sur le Système Nerveux Central) to J.-C.L. and R.R.; and by the CIHR main operating fund to R.R. (MOP-14137) and J.-C.L. (MOP-10848). A.P. was a Long-Term Fellow of the Human Frontier Science Program Organization; R.R. was a Chercheur-National of the FRSQ; K.K.M. held the Canada Research Chair in Molecular Control of Synaptic Structure (Tier II); and J.-C.L. held the Canada Research Chair in Cellular and Molecular Neurophysiology (Tier I).

Received: October 22, 2010
Revised: May 9, 2011
Accepted: July 9, 2011
Published online: August 18, 2011

REFERENCES

Araque, A., Parpura, V., Sanzgiri, R.P., and Haydon, P.G. (1999). Tripartite synapses: glia, the unacknowledged partner. Trends Neurosci. *22*, 208–215.

Araque, A., Martín, E.D., Perea, G., Arellano, J.I., and Buño, W. (2002). Synaptically released acetylcholine evokes Ca2+ elevations in astrocytes in hippocampal slices. J. Neurosci. *22*, 2443–2450.

Ayala, J.E., Niswender, C.M., Luo, Q., Banko, J.L., and Conn, P.J. (2008). Group III mGluR regulation of synaptic transmission at the SC-CA1 synapse is developmentally regulated. Neuropharmacology *54*, 804–814.

Bélair, E.-L., Vallée, J., and Robitaille, R. (2010). In vivo long-term synaptic plasticity of glial cells. J. Physiol. *588*, 1039–1056.

Bergles, D.E., and Jahr, C.E. (1997). Synaptic activation of glutamate transporters in hippocampal astrocytes. Neuron *19*, 1297–1308.

Bushong, E.A., Martone, M.E., Jones, Y.Z., and Ellisman, M.H. (2002). Protoplasmic astrocytes in CA1 stratum radiatum occupy separate anatomical domains. J. Neurosci. *22*, 183–192.

Bushong, E.A., Martone, M.E., and Ellisman, M.H. (2004). Maturation of astrocyte morphology and the establishment of astrocyte domains during postnatal hippocampal development. Int. J. Dev. Neurosci. *22*, 73–86.

Cai, Z., Schools, G.P., and Kimelberg, H.K. (2000). Metabotropic glutamate receptors in acutely isolated hippocampal astrocytes: developmental changes of mGluR5 mRNA and functional expression. Glia *29*, 70–80.

Carter, A.G., and Sabatini, B.L. (2004). State-dependent calcium signaling in dendritic spines of striatal medium spiny neurons. Neuron *44*, 483–493.

Cunha, R.A. (2001). Adenosine as a neuromodulator and as a homeostatic regulator in the nervous system: different roles, different sources and different receptors. Neurochem. Int. *38*, 107–125.

D'Ascenzo, M., Fellin, T., Terunuma, M., Revilla-Sanchez, R., Meaney, D.F., Auberson, Y.P., Moss, S.J., and Haydon, P.G. (2007). mGluR5 stimulates gliotransmission in the nucleus accumbens. Proc. Natl. Acad. Sci. USA *104*, 1995–2000.

Diógenes, M.J., Assaife-Lopes, N., Pinto-Duarte, A., Ribeiro, J.A., and Sebastião, A.M. (2007). Influence of age on BDNF modulation of hippocampal synaptic transmission: interplay with adenosine A2A receptors. Hippocampus *17*, 577–585.

Fellin, T., Pascual, O., Gobbo, S., Pozzan, T., Haydon, P.G., and Carmignoto, G. (2004). Neuronal synchrony mediated by astrocytic glutamate through activation of extrasynaptic NMDA receptors. Neuron *43*, 729–743.

Goldberg, J.H., Tamas, G., Aronov, D., and Yuste, R. (2003). Calcium microdomains in aspiny dendrites. Neuron *40*, 807–821.

Gordon, G.R.J., Iremonger, K.J., Kantevari, S., Ellis-Davies, G.C.R., MacVicar, B.A., and Bains, J.S. (2009). Astrocyte-mediated distributed plasticity at hypothalamic glutamate synapses. Neuron *64*, 391–403.

Gourine, A.V., Kasymov, V., Marina, N., Tang, F., Figueiredo, M.F., Lane, S., Teschemacher, A.G., Spyer, K.M., Deisseroth, K., and Kasparov, S. (2010). Astrocytes control breathing through pH-dependent release of ATP. Science *329*, 571–575.

Grosche, J., Matyash, V., Möller, T., Verkhratsky, A., Reichenbach, A., and Kettenmann, H. (1999). Microdomains for neuron-glia interaction: parallel fiber signaling to Bergmann glial cells. Nat. Neurosci. *2*, 139–143.

Haber, M., Zhou, L., and Murai, K.K. (2006). Cooperative astrocyte and dendritic spine dynamics at hippocampal excitatory synapses. J. Neurosci. *26*, 8881–8891.

Halassa, M.M., and Haydon, P.G. (2010). Integrated brain circuits: astrocytic networks modulate neuronal activity and behavior. Annu. Rev. Physiol. *72*, 335–355.

Halassa, M.M., Fellin, T., Takano, H., Dong, J.-H., and Haydon, P.G. (2007). Synaptic islands defined by the territory of a single astrocyte. J. Neurosci. *27*, 6473–6477.

Hama, K., Arii, T., Katayama, E., Marton, M., and Ellisman, M.H. (2004). Tridimensional morphometric analysis of astrocytic processes with high voltage electron microscopy of thick Golgi preparations. J. Neurocytol. *33*, 277–285.

Henneberger, C., Papouin, T., Oliet, S.H.R., and Rusakov, D.A. (2010). Long-term potentiation depends on release of D-serine from astrocytes. Nature *463*, 232–236.

Holbro, N., Grunditz, A., and Oertner, T.G. (2009). Differential distribution of endoplasmic reticulum controls metabotropic signaling and plasticity at hippocampal synapses. Proc. Natl. Acad. Sci. USA *106*, 15055–15060.

Honsek, S.D., Walz, C., Kafitz, K.W., and Rose, C.R. (2010). Astrocyte calcium signals at Schaffer collateral to CA1 pyramidal cell synapses correlate with the number of activated synapses but not with synaptic strength. Hippocampus. Published online September 29, 2010. 10.1002/hipo.20843.

Kang, J., Jiang, L., Goldman, S.A., and Nedergaard, M. (1998). Astrocyte-mediated potentiation of inhibitory synaptic transmission. Nat. Neurosci. *1*, 683–692.

Latour, I., Gee, C.E., Robitaille, R., and Lacaille, J.C. (2001). Differential mechanisms of Ca2+ responses in glial cells evoked by exogenous and endogenous glutamate in rat hippocampus. Hippocampus *11*, 132–145.

Lujan, R., Nusser, Z., Roberts, J.D., Shigemoto, R., and Somogyi, P. (1996). Perisynaptic location of metabotropic glutamate receptors mGluR1 and mGluR5 on dendrites and dendritic spines in the rat hippocampus. Eur. J. Neurosci. *8*, 1488–1500.

Matsui, K., and Jahr, C.E. (2003). Ectopic release of synaptic vesicles. Neuron *40*, 1173–1183.

Matsui, K., and Jahr, C.E. (2004). Differential control of synaptic and ectopic vesicular release of glutamate. J. Neurosci. *24*, 8932–8939.

Matsui, K., Jahr, C.E., and Rubio, M.E. (2005). High-concentration rapid transients of glutamate mediate neural-glial communication via ectopic release. J. Neurosci. *25*, 7538–7547.

Matthias, K., Kirchhoff, F., Seifert, G., Hüttmann, K., Matyash, M., Kettenmann, H., and Steinhäuser, C. (2003). Segregated expression of AMPA-type glutamate receptors and glutamate transporters defines distinct astrocyte populations in the mouse hippocampus. J. Neurosci. *23*, 1750–1758.

Nett, W.J., Oloff, S.H., and McCarthy, K.D. (2002). Hippocampal astrocytes in situ exhibit calcium oscillations that occur independent of neuronal activity. J. Neurophysiol. *87*, 528–537.

Panatier, A., Theodosis, D.T., Mothet, J.-P., Touquet, B., Pollegioni, L., Poulain, D.A., and Oliet, S.H.R. (2006). Glia-derived D-serine controls NMDA receptor activity and synaptic memory. Cell *125*, 775–784.

Pascual, O., Casper, K.B., Kubera, C., Zhang, J., Revilla-Sanchez, R., Sul, J.-Y., Takano, H., Moss, S.J., McCarthy, K., and Haydon, P.G. (2005). Astrocytic purinergic signaling coordinates synaptic networks. Science *310*, 113–116.

Pasti, L., Volterra, A., Pozzan, T., and Carmignoto, G. (1997). Intracellular calcium oscillations in astrocytes: a highly plastic, bidirectional form of communication between neurons and astrocytes in situ. J. Neurosci. *17*, 7817–7830.

Perea, G., and Araque, A. (2005). Properties of synaptically evoked astrocyte calcium signal reveal synaptic information processing by astrocytes. J. Neurosci. *25*, 2192–2203.

Perea, G., and Araque, A. (2007). Astrocytes potentiate transmitter release at single hippocampal synapses. Science *317*, 1083–1086.

Porter, J.T., and McCarthy, K.D. (1996). Hippocampal astrocytes in situ respond to glutamate released from synaptic terminals. J. Neurosci. *16*, 5073–5081.

Raastad, M., Storm, J.F., and Andersen, P. (1992). Putative Single Quantum and Single Fibre Excitatory Postsynaptic Currents Show Similar Amplitude Range and Variability in Rat Hippocampal Slices. Eur. J. Neurosci. *4*, 113–117.

Rebola, N., Rodrigues, R.J., Lopes, L.V., Richardson, P.J., Oliveira, C.R., and Cunha, R.A. (2005). Adenosine A1 and A2A receptors are co-expressed in pyramidal neurons and co-localized in glutamatergic nerve terminals of the rat hippocampus. Neuroscience *133*, 79–83.

Reid, C.A., Fabian-Fine, R., and Fine, A. (2001). Postsynaptic calcium transients evoked by activation of individual hippocampal mossy fiber synapses. J. Neurosci. *21*, 2206–2214.

Santello, M., Bezzi, P., and Volterra, A. (2011). TNFα controls glutamatergic gliotransmission in the hippocampal dentate gyrus. Neuron *69*, 988–1001.

Serrano, A., Haddjeri, N., Lacaille, J.-C., and Robitaille, R. (2006). GABAergic network activation of glial cells underlies hippocampal heterosynaptic depression. J. Neurosci. *26*, 5370–5382.

Serrano, A., Robitaille, R., and Lacaille, J.-C. (2008). Differential NMDA-dependent activation of glial cells in mouse hippocampus. Glia *56*, 1648–1663.

Smith, M.A., Ellis-Davies, G.C.R., and Magee, J.C. (2003). Mechanism of the distance-dependent scaling of Schaffer collateral synapses in rat CA1 pyramidal neurons. J. Physiol. *548*, 245–258.

Tartaglia, N., Du, J., Tyler, W.J., Neale, E., Pozzo-Miller, L., and Lu, B. (2001). Protein synthesis-dependent and -independent regulation of hippocampal synapses by brain-derived neurotrophic factor. J. Biol. Chem. *276*, 37585–37593.

Todd, K.J., Darabid, H., and Robitaille, R. (2010). Perisynaptic glia discriminate patterns of motor nerve activity and influence plasticity at the neuromuscular junction. J. Neurosci. *30*, 11870–11882.

Ventura, R., and Harris, K.M. (1999). Three-dimensional relationships between hippocampal synapses and astrocytes. J. Neurosci. *19*, 6897–6906.

Volterra, A., and Meldolesi, J. (2005). Astrocytes, from brain glue to communication elements: the revolution continues. Nat. Rev. Neurosci. *6*, 626–640.

Wang, X., Lou, N., Xu, Q., Tian, G.-F., Peng, W.G., Han, X., Kang, J., Takano, T., and Nedergaard, M. (2006). Astrocytic Ca2+ signaling evoked by sensory stimulation in vivo. Nat. Neurosci. *9*, 816–823.

Witcher, M.R., Kirov, S.A., and Harris, K.M. (2007). Plasticity of perisynaptic astroglia during synaptogenesis in the mature rat hippocampus. Glia *55*, 13–23.

Yang, Y., Ge, W., Chen, Y., Zhang, Z., Shen, W., Wu, C., Poo, M., and Duan, S. (2003). Contribution of astrocytes to hippocampal long-term potentiation through release of D-serine. Proc. Natl. Acad. Sci. USA *100*, 15194–15199.

Yuste, R., and Denk, W. (1995). Dendritic spines as basic functional units of neuronal integration. Nature *375*, 682–684.

Zhang, Q., Fukuda, M., Van Bockstaele, E., Pascual, O., and Haydon, P.G. (2004). Synaptotagmin IV regulates glial glutamate release. Proc. Natl. Acad. Sci. USA *101*, 9441–9446.